



# Mass spectrometric study of the oxygen potential at the $\text{UO}_{2-x}$ –U(l) phase limit

M. Baïchi<sup>a</sup>, C. Chatillon<sup>b,\*</sup>, C. Guéneau<sup>c</sup>, J. Le Ny<sup>c</sup>

<sup>a</sup> DRN/DECISECII/LARA, CEA Grenoble, 17 Rue des Martyrs, Grenoble F-38054, France

<sup>b</sup> Laboratoire de Thermodynamique et de Physico-Chimie Métallurgiques, (UMR 5614, CNRS-INPG/UJF) – ENSEEG, Domaine Universitaire BP.75, Saint Martin d'Hères F-38402, France

<sup>c</sup> DCC/DPE/SPCP/LEPCA, CEA Saclay, Gif-sur-Yvette cedex F-91191, France

Received 10 December 2001; accepted 29 January 2002

## Abstract

Activity measurements of  $\text{UO}_2$  at the phase boundary U(l)– $\text{UO}_{2-x}$  have been performed by high temperature mass spectrometry in order to solve discrepancies observed in earlier works. The direct measurement of the  $\text{UO}_2$  activity was performed using the multiple Knudsen cell method and a special collimation device in order to (i) circumvent any usual calibration methods (ii) discard any earlier observed parasitic contributions in this system. The oxygen potential is then directly calculated on the basis of pure  $\text{UO}_2$ (s) accurate thermodynamic data for the diphasic U(l)– $\text{UO}_{2-x}$  domain in the 2000–2250 K range. © 2002 Published by Elsevier Science B.V.

## 1. Introduction

The oxygen potential in the diphasic  $\text{UO}_{2-x}$ (substoichiometric solidus)–U(liquid saturated with oxygen) has been already determined in two mass spectrometric works [1–4] performed with effusion cells. The partial pressures of U(g), UO(g) and  $\text{UO}_2$ (g) over this diphasic domain were measured either as a function of temperature [1,3] or at constant temperature in an isothermal run [2,3] as a function of composition.

In the first method, partial pressure of oxygen is deduced from equilibria involving the U(g), UO(g) and  $\text{UO}_2$ (g) species for which conventional calibration procedures were used based on effusion mass loss (i) of a reference and in situ material (Ag) evaporated at the beginning of the experiment (ii) of the U +  $\text{UO}_2$  system itself (iii) or of the U +  $\text{UO}_2$  system evaporated in another device fitted with a condensation target. Whatever are these methods, the presence in the gas phase of three molecules, U(g), UO(g) and  $\text{UO}_2$ (g) the partial pressures

of which are within one order of magnitude, needs the evaluation of their relative sensitivities, that is in fact their relative ionization cross-sections and detection yields. All these estimates give rise to uncertainties. As a matter of fact, the deduced pressures are different by a factor of three between Ackermann et al. [1] and Drowart et al. [12].

The second method uses the fact that UO(g) is the main component of the gas phase, and consequently any starting composition of the condensed phase with  $\text{O}/\text{U} > 1$ , will have an evolution of composition by effusion loss toward the  $\text{UO}_{2-x}$  congruent composition for vaporization [2,3]. In such experiments, and as long as the mass spectrometer sensitivity is kept constant, the relative evolution of the U(g), UO(g) and  $\text{UO}_2$ (g) pressures may be recorded with a better accuracy. The comparison of  $p(\text{UO}_2)$  over the diphasic U(l) +  $\text{UO}_{2-x}$  and for the congruent  $\text{UO}_{2-x}$  (for which  $2-x$  is close to 2) shows that there is a slight decrease of the  $\text{UO}_2$  activity for the phase boundary at temperature above 2000 K when compared to pure  $\text{UO}_2$ (s) or congruent  $\text{UO}_{2-x}$ (s).

A third method was used [3] to intercompare directly these two pressures of  $\text{UO}_2$ (g), that is the twin cell

\* Corresponding author.

E-mail address: chatillon@ltpcm.inpg.fr (C. Chatillon).

method [5]: two effusion cells, located in a same isothermal block are loaded with the U + UO<sub>2-x</sub> mixture and with pure UO<sub>2</sub>(s). The partial pressures of UO<sub>2</sub>(g) are directly compared to determine the UO<sub>2</sub> activity

$$a_{\text{UO}_2} = \frac{p(\text{UO}_2)(\text{U} + \text{UO}_{2-x})}{p(\text{UO}_2)(\text{pure UO}_2)} \quad (1)$$

and using the basic mass spectrometric relation [5,6]

$$p_i S_i = I_i T$$

in which  $S_i$  is the sensitivity,  $I_i$  the measured ionic intensity of the  $i$  species, and  $T$  the cell temperature, we deduce for a constant  $S_i$  during each set of measurements

$$a_{\text{UO}_2} = \frac{I_{\text{UO}_2, \text{mixture}}}{I_{\text{UO}_2, \text{pure}}} \quad (2)$$

Discrepancies obtained between works performed according to the first method [1–4] were partly solved by the second and third methods [2,3]. The present work has been performed in order to propose definitely correct values of oxygen partial pressures for the diphasic U–UO<sub>2-x</sub> domain. The method used is the multiple cell method [7,8] which is a development of the twin cell method [2,3]. This method was chosen because the mass spectrometric sensitivity has not to be determined but is permanently at the disposal of the experimenter via a reference sample in one cell of the multiple cell device.

## 2. Experimental technique

The experimental device used has been recently described [9] altogether with specific requirements – namely the use of a restricted collimation device [10], the main objective of which was to discard any possibilities of parasitic molecular flows detection. Indeed some of them were previously detected and analyzed for the U(l) or U(l) + UO<sub>2</sub> system [2,3]. In our study, and when moving the cells to locate the different effusion orifices on the mass spectrometer ion source axis, we effectively observed (Fig. 1) these parasitic surface (orifice neighbourhood) vaporizations that may also vary with temperature since any effusion process enhances steady-state parasitic flows in the hot volume of the furnace (thermal shields, resistors...). The less sharp profiles observed in this study when compared to the previous one on the UO<sub>2</sub>–ZrO<sub>2</sub> pseudobinary system [9] attest an increase of the parasitic flows due to probably large surface diffusion or creeping due to liquid uranium along the orifice walls, as already observed [11]. The measurement of the lone and genuine effusion flow is then performed within the observed plateau (see Fig. 1) without any contribution of parasitic flows [10].

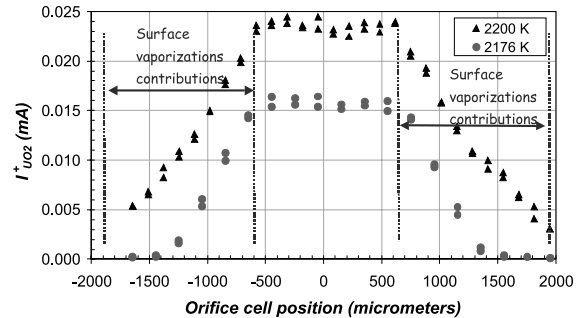


Fig. 1. Observation of external surface vaporizations when moving the effusion orifice in a plane perpendicular to the ion source axis. In order to discard these contributions, the measurements are performed on the central plateau using a restricted collimation device.

Effusion cells (crucible + lid) were machined in tungsten, and four of these located in a tantalum envelope as already described [9]. The ratio  $sC/S$ , where  $s$  is the orifice cross-section,  $C$  the Clausing coefficient and  $S$  the cell cross-section was equal to  $9.5 \times 10^{-3}$ . Temperature measurements were performed with W/Re thermocouples. The samples were made of pure U (chips) mixed with UO<sub>2</sub> fine powder (same as in Ref. [9]), in order to facilitate the attainment of equilibrium since UO<sub>2</sub> has to become UO<sub>2-x</sub> (phase limit composition) meanwhile U(l) cannot dissolve large quantities of oxygen [12]. Different overall compositions in the U–UO<sub>2</sub> system were chosen (O/U = 0.34, 0.35, 0.45 and 0.5) in order to check equilibrium conditions for vaporization. The direct intercomparison of vapors of these compositions in the four cells never showed any appreciable differences in the vapor pressures of U(g), UO(g) or UO<sub>2</sub>(g). These measurements within the same diphasic U(l) + UO<sub>2</sub>(s), as well as pure UO<sub>2</sub>(s) or preliminary checks with gold loaded in the four cells showed that there were no significant temperature gradients in our Ta envelope. The observed standard deviations ( $\sim \pm 5\%$ ) were therefore attributed to the mass spectrometer (peak matching) and its detection system (SEM and analogic detection). We observed in the activity measurements quite the same standard deviations that we propose to choose as the uncertainty (see for measurements the procedure in Ref. [9]).

## 3. Experimental results and discussion

Results obtained for our four overall compositions are presented in Fig. 2 and compared to preceding values of the UO<sub>2</sub> activity as determined by Drowart et al. [2] Pattoret [3] and Ackermann et al. [1,4]. Our present determinations agree with those of Drowart et al. and Pattoret and the activity evolution with temperature

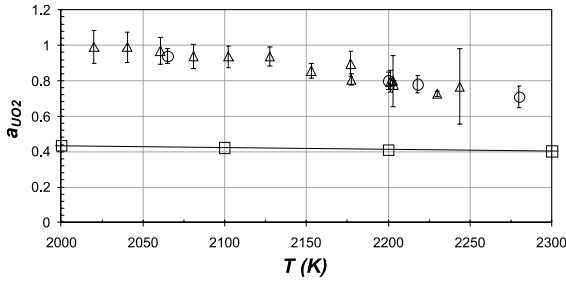


Fig. 2. Results of our  $\text{UO}_2$  activity measurements with the multiple cell device ( $\Delta$ ), and comparison with literature: ( $\circ$ ) Pattoret [3] with a twin cell device, ( $\square$ ) Ackermann et al. [1,4] with a conventional effusion method. When mentioned, the error bars correspond to the standard deviation.

seems more reasonable when taking into account the phase diagram shape i.e. a substoichiometric domain  $\text{UO}_{2-x}$  more extended at  $T > 2000$  K, and a very small

$$\delta \overline{\Delta G}_{\text{O}_2} = \sqrt{[\delta(\Delta_f H_{298}^0(\text{UO}_{2,s}))]^2 + [T\delta(\Delta S_{298}(\text{UO}_2))]^2 + [\delta\Delta H_{\text{fus}}(\text{U})]^2 + \left[RT \frac{\delta a_{\text{UO}_2}}{a_{\text{UO}_2}}\right]^2 + \left[RT \frac{\delta x_{\text{U}}}{x_{\text{U}}}\right]^2}. \quad (7)$$

oxygen solubility in liquid Uranium [12]. This last point will be discussed later in a critical review of the phase diagram data [13].

Conversely to direct measurements of partial pressures of the  $\text{U}(\text{g})$ ,  $\text{UO}(\text{g})$  and  $\text{UO}_2(\text{g})$ , the activity determination of  $\text{UO}_2$  can be directly related to the oxygen partial pressure in the diphasic  $\text{U}(\text{l}) + \text{UO}_{2-x}$  via a single reaction,



in which no calibration for gaseous species are needed. The equilibrium constant,

$$K_p = \frac{a(\text{U}, \text{l})p_{\text{O}_2}(\text{g})}{a_{\text{UO}_{2(\text{ss})}}}, \quad (4)$$

is known from the Gibbs energy of formation of  $\text{UO}_2(\text{s}, \text{stoichiometric})$  [14], as compiled from independent measurements,

$$RT \ln K_p = -\Delta_f G_T^0(\text{UO}_2, \text{s}). \quad (5)$$

Finally,  $p_{\text{O}_2}$  or the partial Gibbs energy of oxygen are deduced from relations (4) and (5) as

$$\overline{\Delta G}_{\text{O}_2} = \Delta_f G_T^0(\text{UO}_2, \text{s}) + RT \ln \frac{a_{\text{UO}_2}}{a_{\text{U}}} \quad (6)$$

relation in which  $a_{\text{U}} = x_{\text{U}}$  according to Raoult's law and a very small solubility of oxygen [12]. The uncertainty generated by our measurements and the chosen references are calculated according to the propagation law of errors [15] to be

The origin of the uncertainties are presented in Table 1. The final results of oxygen potential on partial Gibbs energy altogether with their associated uncertainties are presented in Table 2.

#### 4. Conclusion

The activity of  $\text{UO}_2$  at the substoichiometric solidus of  $\text{UO}_{2-x}$  has been measured by the multiple cell method – a development of the earlier so-called twin cell method – and with intercomparison of the partial pressures of  $\text{UO}_2(\text{g})$  at this phase boundary and for pure or con-

Table 1

Reference data and their associated overall uncertainties as used to calculate the oxygen potential (according to relations (6) and (7)) for the diphasic  $\text{U}(\text{l})\text{--}\text{UO}_{2-x}(\text{s})$

Thermodynamic functions	Data and uncertainty	Reference
$\Delta_f H^0(\text{UO}_{2,s}, 298.15 \text{ K})$	$-1085.0 \pm 1.0 \text{ kJ mol}^{-1}$	[16]
$S^0(\text{UO}_{2,s}, 298.15 \text{ K})$	$77.03 \pm 0.20 \text{ J K}^{-1} \text{ mol}^{-1}$	[16]
$S^0(\text{U}, s, 298.15 \text{ K})$	$50.20 \pm 0.20 \text{ J K}^{-1} \text{ mol}^{-1}$	[16]
$\delta(\Delta_{\text{fus}} H^0(\text{U}, s \rightarrow \text{l}))$	$8.52 \text{ kJ mol}^{-1}$ at $1405 \pm 2 \text{ K}$	[17]
$\delta S(\text{U}, \text{l})$	$\delta S_{298}^0(\text{U}, s) + \delta \int (C_p^0/T) dT + \delta(\Delta_{\text{fus}} H_U^0/T_{\text{fus}})$ or $\pm 0.20 \pm 0^a \pm 0.006 \text{ J K}^{-1} \text{ mol}^{-1}$	[16,17]
$S^0(\text{O}_2, \text{g}, 298.15 \text{ K})$	$206 \pm 0.8 \text{ J K}^{-1} \text{ mol}^{-1}$	[18]
$\delta a_{\text{UO}_2}/a_{\text{UO}_2}$	Standard deviation	This work
$\delta x_{\text{U}(\text{liq.})}/x_{\text{U}(\text{liq. rat.0})}$	$\pm 0.01/x_{\text{U}}$	[13]

<sup>a</sup> This value is set at zero in the thermodynamic tables because the uncertainty is reported on  $S^0$  and  $\Delta_f H^0$  or  $\Delta_{\text{fus}} H^0$ .

Table 2

Oxygen potentials as calculated from our  $\text{UO}_2$  activity measurements for the diphasic  $\text{U(l)} + \text{UO}_{2-x}\text{(s)}$  and their uncertainty range

$T$ (K)	$\Delta G_{\text{O}_2}$ (J mol <sup>-1</sup> )	$p(\text{O}_2/\text{bar})$
2177 ± 10	-713 819 ± 2885	$(7.47 \pm 1.19) \times 10^{-18}$
2201	-711 904 ± 2698	$(1.27 \pm 0.19) \times 10^{-17}$
2203	-711 600 ± 2698	$(1.34 \pm 0.20) \times 10^{-17}$
2244	-705 531 ± 2704	$(3.78 \pm 0.55) \times 10^{-17}$
2020	-738 494 ± 2878	$(8.01 \pm 1.37) \times 10^{-20}$
2040	-735 105 ± 2851	$(1.51 \pm 0.25) \times 10^{-19}$
2061	-732 069 ± 2824	$(2.80 \pm 0.46) \times 10^{-19}$
2081	-729 140 ± 2798	$(4.99 \pm 0.81) \times 10^{-19}$
2102	-725 601 ± 2772	$(9.32 \pm 1.48) \times 10^{-19}$
2127	-721 367 ± 2745	$(1.93 \pm 0.30) \times 10^{-18}$
2153	-718 692 ± 2722	$(3.66 \pm 0.55) \times 10^{-18}$
2178	-715 659 ± 2706	$(6.87 \pm 1.03) \times 10^{-18}$
2203	-712 066 ± 2698	$(1.31 \pm 0.19) \times 10^{-17}$
2230	-708 810 ± 2699	$(2.50 \pm 0.36) \times 10^{-17}$

gruent  $\text{UO}_2\text{(s)}$ . This direct measurement that does not need conventional calibration procedures of the mass spectrometer leads to more reliable determinations and consequently better accuracy. Discrepancies between earlier works are solved and a better selection of original data is now possible in view of further optimization of thermodynamic and phase diagram data of the U–O system.

### Acknowledgements

The authors acknowledge Electricité de France for sponsoring this study.

### References

- [1] R.J. Ackermann, E.G. Rauh, M.S. Chandrasekhariah, J. Phys. Chem. 73 (1969) 762.
- [2] J. Drowart, A. Pattoret, S. Smoes, Proc. Brit. Ceram. Soc. 8 (1967) 67.
- [3] A. Pattoret, PhD, Université Libre de Bruxelles, 1969, p. 249.
- [4] R.J. Ackermann, E.G. Rauh, M.H. Rand, A re-determination and re-assessment of the thermodynamics of sublimation of uranium dioxide, in: 5th International Symposium on Thermodynamics of Nuclear Materials, 29 Jan–2 Feb, AIEA, Jülich, Germany, 1979.
- [5] C. Chatillon, A. Pattoret, J. Drowart, High Temp. High Press. 7 (1975) 119.
- [6] C. Chatillon, M. Allibert, A. Pattoret, Characterization of High Temperature Vapors and Gases, NBS Sp. Pub. 561/1, NIST, Gaithersburg, MD, USA, 1979, p. 181.
- [7] C. Chatillon, Electrochem. Soc. Proc. 97 (1997) 648.
- [8] C. Chatillon, L.F. Malheiros, P. Rocabois, M. Jeymond, High Temp. High Press. 34 (2002) 213.
- [9] M. Baïchi, C. Chatillon, C. Guéneau, S. Chatain, J. Nucl. Mater. 294 (2001) 84.
- [10] P. Morland, P. Rocabois, C. Chatillon, High Temp. Mater. Sci. 37 (1997) 167.
- [11] A. Pattoret, J. Drowart, S. Smoes, Trans. Far. Soc. 65 (1969) 98.
- [12] R.K. Edwards, A.E. Martin, in: Thermodynamics, IAEA, Vienna, Austria, 1966, p. 423.
- [13] M. Baïchi, PhD, Institut National Polytechnique de Grenoble, 24 Septembre 2001, Grenoble, France.
- [14] M.H. Rand, R.J. Ackermann, F. Gronvold, F.L. Oetting, A. Pattoret, Rev. Int. Hautes Temper. Réfract. Fr. 15 (1978) 355.
- [15] F. Rossini, Assignment of Uncertainties to Thermochemical Data in Experimental Thermochemistry, Interscience, New York, 1956, p. 297.
- [16] J.D. Cox, D.D. Wagman, V.A. Medvedev, in: CODATA Key Values for Thermodynamics, Hemisphere, New York, 1989, p. 26.
- [17] R. Hultgren, P.D. Desai, D.T. Hawkins, M. Gleiser, K.K. Kelley, Selected Values of the Thermodynamic Properties of the Elements, American Society for Metals, Metals Park, OH, 1973.
- [18] M.W. Chase Jr., J. Phys. Chem. Ref. Data, Monograph no. 9, NIST-JANAF Thermochemical Tables, 4th Ed., NIST, Gaithersburg, MD, USA, 1998.